# Effect of Transmural Transport Properties on Atheroma Plaque Formation and Development

M. Cilla,[1] M. A. Martínez,[2,3] and E. Peña[2,3]

[1]Julius Wolff Institute, Charité - Universitätsmedizin Berlin, Berlin, Germany; [2]Applied Mechanics and Bioengineering Group, Aragón Institute of Engineering Research (I3A), University of Zaragoza, María de Luna, 3, 50018 Zaragoza, Spain; and [3]Centro de Investigación en Red en Bioingeniería, Biomateriales y Nanomedicina, Zaragoza, Spain

**Abstract**—We propose a mathematical model of atheroma plaque initiation and early development in coronary arteries using anisotropic transmural diffusion properties. Our current approach is on the process on plaque initiation and intimal thickening rather than in severe plaque progression and rupture phenomena. The effect of transport properties, in particular the anisotropy of diffusion properties of the artery, on plaque formation and development is investigated using the proposed mathematical model. There is not a strong influence of the anisotropic transmural properties on LDL, SMCs and collagen distribution and concentrations along the artery. On the contrary, foam cells distribution strongly depends on the value of the radial diffusion coefficient of the substances $D^{r}$ and the ratio $\gamma = D^{z}_{i,w}/D^{r}_{i,w}$. Decreasing $\gamma$ or diffusion coefficients ratio means a higher concentration of the foam cells close to the intima. Due to the fact that foam cells concentration is associated to the necrotic core formation, the final distribution of foam cells is critical to evolve into a vulnerable or fibrotic plaque.

**Keywords**—Atheroma plaque, Convection–diffusion–reaction equations, LDL transport, Growth.

## INTRODUCTION

Atherosclerosis is the process in which plaques—consisting of deposits of cholesterol and other lipids, calcium and large inflammatory cells called macrophages—are built up in the walls of the arteries causing narrowing, hardening of the arteries and loss of elasticity. The mechanical factors which could initiate the atherosclerosis lesion has been widely explored by many authors.[11,30,38,51,57] Cyclic stretch, laminar and oscillatory shear stress, effects of vessel compliance, curvature, pulsatile blood flow or cardiac motion are considered the main mechanical triggers of atherosclerosis initiation.[30]

The fundamental cause of plaque development is believed to be the abnormal enlargement of the intima by the infiltration and accumulation of macromolecules such as lipoproteins and the associated cellular and synthetic reactions.[28] This suggests that the macromolecular transport in the arterial wall must have some impact on the initiation and development of atherosclerosis.[59] Therefore, zones of elevated LDL tend to correspond to areas of atherosclerotic lesion development and intimal thickening, and such zones also tend to have "abnormal" WSS patterns.[38] The endothelium, which is the internal lining of the entire cardiovascular system, is uniquely positioned to be a sensor, responding and transducing these hemodynamic signals.[36] Fatty streaks, the earliest detectable lesions in atherosclerosis, contain macrophage-derived foam cells that differentiate from recruited blood monocytes. Monocytes are recruited to tissues *via* constitutive signals and in response to inflammatory mediators.[37] More advanced atherosclerotic lesions, called fibro-fatty plaques, are the result of continued monocyte recruitment, together with smooth muscle cell migration and proliferation.[49] In addition, some chemokineses that can act as potent mediators of monocyte and SMC migration and macrophage differentiation are expressed in human atherosclerotic lesions.[2,65]

Several authors analyzed the macromolecular transport of the LDL along the arterial wall.[1,12,28,29,44,52,60] A number of works[12,23] indicate that the arterial transport properties are controlled by the microstructure of the layers of the arterial wall. Due to the structure of the arterial wall, there are one or two-orders of magnitude

Address correspondence to E. Peña, Applied Mechanics and Bioengineering Group, Aragón Institute of Engineering Research (I3A), University of Zaragoza, María de Luna, 3, 50018 Zaragoza, Spain. Electronic mail: fany@unizar.es

difference between the diffusion properties in axial and radial direction.[25,35] However, most of them considered the isotropic diffusion properties.

In a previous work, a computational *model* based on reaction–*convection*–diffusion equations coupled with blood-wall mass transport of the main biological species which lead to atheroma plaque development was presented.[13] These biological agents and substances were LDL, oxidized LDL, monocytes, macrophages, foam cells, smooth muscle cells, cytokines and collagen. The dependence of fluid and mass transport through the endothelium on local blood flow characteristics was modeled using a three pore model correlated to WSS.[44] In this study based on the aforementioned mathematical model, the impact due to changes in the microstructure which results in a variation of transport properties is analyzed. In particular, the effects of the changes of transmural transport properties on the atheroma plaque development are studied based on our new mathematical model.

## GOVERNING EQUATIONS

The endothelium consists of a single layer of endothelial cells while the arterial wall is usually considered as a porous medium.[16] We modeled the transport phenomena through a homogeneous wall where the arterial wall is approximated by a simple homogeneous media layer.[28] Mass transfer across the arterial wall occurs *via* two main mechanisms: convection associated with the gradient of pressures which promotes transmural flow and mass diffusion caused by concentration gradients. Different substances and species are transferred between the lumen and the vessel wall and react between them. The main phenomena modeled using the diffusion–convection–reaction equations are: the monocyte ($m$) transmigration and later differentiation into macrophages ($M$); the *LDL* accumulation and further oxidation; the ingest of oxidized LDL ($LDL_{ox}$) by the macrophages and their apoptosis, leading to foam cells ($F$); the differentiation of contractile ($S_c$) into synthetic ($S_s$) smooth muscle cells due to cytokines ($c$), the migration of synthetic smooth muscle cells and their secretion of collagen ($G$). Figure 1 schematic shows the considered substances and cells in the atheroma plaque growth process as well as their interaction between them.

### *Lumen*

The blood flow was assumed to be steady, incompressible, laminar, Newtonian and, hence, governed by the Navier–Stokes equation ($1_1$) and the continuity equation ($1_2$)

$$(\boldsymbol{u}_\mathrm{l}\cdot\nabla)\boldsymbol{u}_\mathrm{l}-\mu_\mathrm{b}\Delta\boldsymbol{u}_\mathrm{l}+\frac{1}{\rho_\mathrm{b}}\nabla p_\mathrm{l}=0,\quad \nabla\cdot\boldsymbol{u}_\mathrm{l}=0. \tag{1}$$

The subscript l is used to represent the lumen, then, $\boldsymbol{u}_\mathrm{l}$ is the velocity vector field in the lumen, $p_\mathrm{l}$ is the lumen pressure, and $\mu_\mathrm{b}$ and $\rho_b$ the blood density and dynamic viscosity, respectively.

The LDL and monocyte transport in the blood fluid domain along the artery lumen is governed by the convection–diffusion equation:

$$\underbrace{\nabla\cdot(-D_{\mathrm{LDL,l}}\nabla C_{\mathrm{LDL,l}})}_{\text{Diffusion}}+\underbrace{\boldsymbol{u}_\mathrm{l}\cdot\nabla C_{\mathrm{LDL,l}}}_{\text{Convection}}=0, \tag{2}$$

$$\underbrace{\nabla\cdot(-D_{\mathrm{m,l}}\nabla C_{\mathrm{m,l}})}_{\text{Diffusion}}+\underbrace{\boldsymbol{u}_\mathrm{l}\cdot\nabla C_{\mathrm{m,l}}}_{\text{Convection}}=0, \tag{3}$$

where $D_{\mathrm{LDL,l}}$ and $D_{\mathrm{m,l}}$ are the LDL and monocytes diffusion coefficient in the lumen blood flow and $C_{\mathrm{LDL,l}}$ and $C_{\mathrm{m,l}}$ are the LDL and monocyte concentration respectively.

### *Arterial Wall*

*Substances*

The diffusion and convection equations for the substances through the artery wall can be modeled as

$$\frac{\partial C_{\mathrm{LDL,w}}}{\partial t}+\underbrace{\nabla\cdot(-D_{\mathrm{LDL,w}}\nabla C_{\mathrm{LDL,w}})}_{\text{Diffusion}}+\underbrace{\boldsymbol{u}_\mathrm{w}\cdot\nabla C_{\mathrm{LDL,w}}}_{\text{Convection}}=\underbrace{-d_{\mathrm{LDL}}C_{\mathrm{LDL,w}}}_{\text{LDLoxidation}}, \tag{4}$$

$$\frac{\partial C_{\mathrm{LDL_{ox,w}}}}{\partial t}+\underbrace{\nabla\cdot(-D_{\mathrm{LDL_{ox,w}}}\nabla C_{\mathrm{LDL_{ox,w}}})}_{\text{Diffusion}}+\underbrace{\boldsymbol{u}_\mathrm{w}\cdot\nabla C_{\mathrm{LDL_{ox,w}}}}_{\text{Convection}}=\underbrace{d_{\mathrm{LDL}}C_{\mathrm{LDL,w}}}_{\text{OxidatedfromLDL}}-\underbrace{\mathrm{LDL_{oxr}}C_{\mathrm{LDL_{ox,w}}}C_{\mathrm{M,w}}}_{\text{Uptakenbymacrophages}}, \tag{5}$$

$$\frac{\partial C_{c,w}}{\partial t} + \underbrace{\nabla \cdot (-D_{c,w} \nabla C_{c,w})}_{\text{Diffusion}} + \underbrace{\boldsymbol{u}_w \cdot \nabla C_{c,w}}_{\text{Convection}} = \underbrace{-d_c C_{c,w}}_{\text{Degradation}} + \underbrace{C_r C_{LDL_{ox},w} C_{M,w}}_{\text{Production}}, \tag{6}$$

$$\frac{\partial C_{G,w}}{\partial t} + \underbrace{\nabla \cdot (-D_{G,w} \nabla C_{G,w})}_{\text{Diffusion}} + \underbrace{\boldsymbol{u}_w \cdot \nabla C_{G,w}}_{\text{Convection}} = \underbrace{G_r C_{S_s,w}}_{\text{Secreted}} - \underbrace{d_G C_{G,w}}_{\text{Degradation}}, \tag{7}$$

where $C_{i,w}$ and $D_{i,w}$ are the concentration in the artery wall and the diffusive coefficient in the plasma of the $i$ substance, respectively.

Apart from the diffusive and convective terms of Eq. (4), the term relating to the reaction part, $d_{LDL}C_{LDL,w}$, corresponds to the LDL oxidation formation, indicating the concentration of LDL per second which is oxidized. $d_{LDL}$ is the degradation rate of LDL. The $D_{LDL_{ox,w}}$ value has been considered as similar to that used for the LDL substance by Prosi *et al.*[46] $d_{LDL}C_{LDL,w}$ models the oxidized LDL process from the LDL. Finally, the quantity of LDL uptake captured by the macrophages per second $\left(\frac{mol}{m^3 s}\right)$ is defined by the second term on the right hand side of Eq. (5), where $C_{M,w}$ is the concentration of macrophages and $LDL_{oxr}$ is the rate of LDL uptake by each macrophage. $d_c$ is

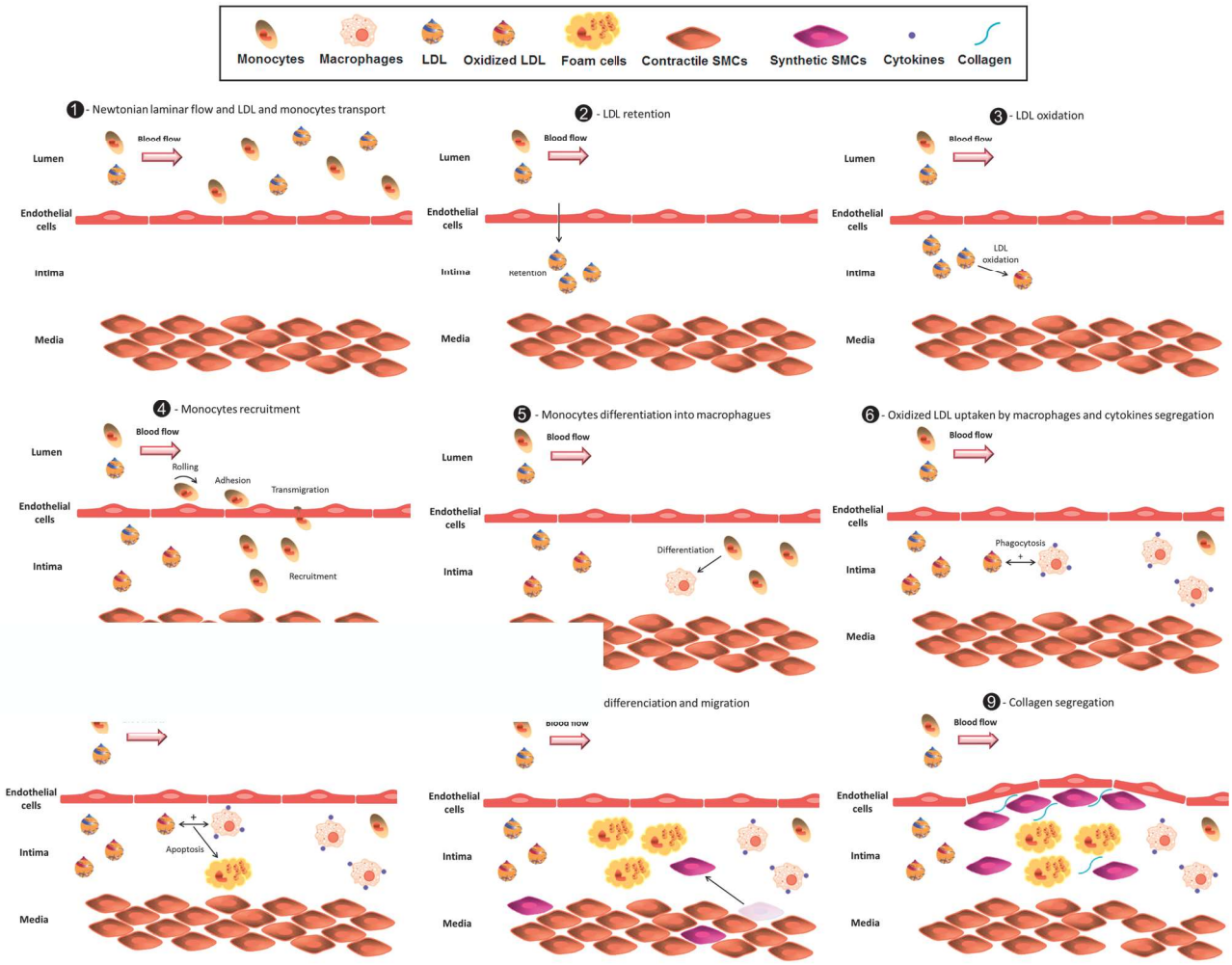


**FIGURE 1. Schematic representation of the different considered processes, cells and substances into the atheroma plaque growth model.**

the degradation rate of cytokines, and $C_r$ the production ratio of cytokines due to the presence of oxidized LDL and macrophages.[50] Moreover, since macrophages are responsible for cytokine secretion due to the oxidized LDL, the concentrations of both species are included in the cytokine production term. The collagen is secreted at the rate $G_r$, and degraded at the rate $d_G$. The natural degradation of the collagen as the age increases has not been taken into account. Diffusion and convection effects of cytokines have been disregarded, because it was considered that cytokines are retained in the macrophage membrane.[8]

*Cells*

Due to the size of the cells, the convection term has been disregarded.[5,6] The diffusion and reaction governed equations for the cells are

Therefore, the last term on the right hand side of Eq. (9) corresponds to the chemotaxis of the monocytes due to the presence of oxidized LDL. The gaussian function tends to 0 when the monocyte concentration is bigger than $C^{th}_{M,w}$, a threshold for monocyte concentration which is set to the same value as the monocyte blood concentration. The first term of right side on Eq. (8) corresponds to the monocytes which have been differentiated into macrophages; and the second term models the foam cell formation. The foam cell formation depends on the quantity of oxidized LDL ingested by the macrophages ($LDL_{oxr} C_{M,w} C_{LDL_{ox,w}}$), which has been multiplied and divided by the constants $M_{r1}$ and $M_{r2}$. The former corresponds to the oxidized LDL concentration per second that a single macrophage should ingest to convert into a foam cell. The latter refers to the rate of foam cell formation per second depending on the

$$\frac{\partial C_{m,w}}{\partial t} + \underbrace{\nabla \cdot (-D_{m,w} \nabla C_{m,w})}_{\text{Diffusion}} + \underbrace{\cancel{\boldsymbol{u}_w \cdot \nabla C_{m,w}}}_{\text{Convection}} = - \underbrace{d_m C_{m,w}}_{\text{Macrophage differentiation}} - \underbrace{m_d C_{m,w}}_{\text{Apoptosis}} + \underbrace{C_{m,w} C_{LDL\ ox,w} \exp \frac{-C^2_{m,w}}{2C^{th\ 2}_{m,w}}}_{\text{Chemotaxis}}, \tag{8}$$

$$\frac{\partial C_{M,w}}{\partial t} + \underbrace{\nabla \cdot (-D_{M,w} \nabla C_{M,w})}_{\text{Diffusion}} + \underbrace{\cancel{\boldsymbol{u}_w \cdot \nabla C_{M,w}}}_{\text{Convection}} = \underbrace{d_m C_{m,w}}_{\text{Differenciate from monocytes}} - \underbrace{\frac{M_{r1}}{M_{r2}} LDL_{oxr} C_{M,w} C_{LDL\ ox,w}}_{\text{Apoptosis to foam cells}}, \tag{9}$$

$$\frac{\partial C_{F,w}}{\partial t} + \underbrace{\cancel{\nabla \cdot (-D_{F,w} \nabla C_{F,w})}}_{\text{Diffusion}} + \underbrace{\cancel{\boldsymbol{u}_w \cdot \nabla C_{F,w}}}_{\text{Convection}} = \underbrace{\frac{M_{r1}}{M_{r2}} LDL_{oxr} C_{M,w} C_{LDL\ ox,w}}_{\text{Apoptosis from macrophages}}, \tag{10}$$

$$\frac{\partial C_{S_c,w}}{\partial t} + \underbrace{\cancel{\nabla \cdot (-D_{S_c,w} \nabla C_{S_c,w})}}_{\text{Diffusion}} + \underbrace{\cancel{\boldsymbol{u}_w \cdot \nabla C_{S_c,w}}}_{\text{Convection}} = \underbrace{-C_{S_c,w}(1 - \exp \frac{-S_r C_{c,w}}{C^{th}_{c,w}})}_{\text{Differentiation}}, \tag{11}$$

$$\frac{\partial C_{S_s,w}}{\partial t} + \underbrace{\cancel{\nabla \cdot (-D_{S_s,w} \nabla C_{S_s,w})}}_{\text{Diffusion}} + \underbrace{\cancel{\boldsymbol{u}_w \cdot \nabla C_{S_s,w}}}_{\text{Convection}} = \underbrace{C_{S_c,w}(1 - \exp \frac{-S_r C_{c,w}}{C^{th}_{c,w}})}_{\text{Differentiation}} + \underbrace{C_{S_s,w} \frac{C_{c,w}}{C^{th}_{c,w}} m_{S_s}}_{\text{Chemotasis}}, \tag{12}$$

where $C_{i,w}$ and $D_{i,w}$ are the concentration and diffusive coefficients of the different cell populations, respectively. $d_m$ is the constant rate that modulates the monocyte differentiation. The second term of the right side on Eq. (9) represents the monocytes natural death. The monocytes undergo random motion, are chemotactically attracted to the chemicals in the presence of oxidized LDL and grow up to a maximal value $C^{th}_{M,w}$. macrophage concentration. The first reaction term of Eq. (10) corresponds to the macrophage apoptosis, whose constant has already been defined. Initially, SMCs were assumed to be in a contractile phenotype. The presence of cytokines modulates their differentiation towards a synthetic phenotype by the differentiation rate of these cells due to the presence of cytokines.[9] The contractile smooth cell differentiation

is modeled as a reverse sigmoid function where at the maximum concentration of cytokines, $Cc,w^{th}$, the differentiation is maximum. Since the mitosis and death of these cells are regulated by the organism body and both rates tend to be in equilibrium, the proliferation and apoptosis of these cells are not included in the equations. The diffusion of SMCs is disregarded since these cells migrate instead of being spread by diffusion. Finally, synthetic smooth muscle cells are induced into the intima by the chemoattractant (cytokines), being $m_{S_s}$ the migration rate of these cells.[20] Again, the convention of these cells has been disregarded owing to their size, as with other cells included in this model. Moreover, contractile SMCs cells are considered quiescent, and therefore there is no diffusion process. The diffusion of synthetic SMCs is disregarded because these cells migrate instead of being spread by diffusion.[20]

An initial concentration of contractile smooth muscle cells of $29.28 \times 10^{12}$ mol/m$^3$ is defined as the initial condition,[62] and insulation boundary conditions were applied.

### *Transmural Plasma Flow Throughout the Artery Wall*

The transmural velocity vector field $\boldsymbol{u}_w$ in the arterial wall is calculated with Darcy's Law ($13_1$) and the corresponding continuity equation ($13_2$),

$$\boldsymbol{u}_w = \frac{\kappa_w}{\mu_p}\nabla p_w, \quad \frac{\partial(\rho_p \epsilon_p)}{\partial t} + \rho_p \nabla \cdot \boldsymbol{u}_w = 0, \tag{13}$$

where the subscript w is used to represent the artery wall variables, $\kappa_w$ is the Darcian permeability of the arterial wall, $\rho_p$ and $\mu_p$ are the density and dynamic viscosity of the blood plasma, respectively, $p_w$ is the pressure within the arterial wall which is determined by the blood flow simulation along the artery lumen, and $\epsilon_p$ is the porosity of the artery wall.[44]

### *Plaque Formation*

The mass balance for open systems can be written as $\frac{\partial \rho_o^i}{\partial t} = \Pi_i - \nabla \cdot \boldsymbol{M}_i$ where $\rho_o$ is the total density of the tissue in the reference configuration, $\Pi_i$ are the source/sinks and $\boldsymbol{M}_i$ the mass fluxes of the $i$ arbitrary species. $\Pi_i$ are related to migration, proliferation, differentiation and apoptosis of the cells and secretion and degradation of the substances. The concentrations of each species have the property $\rho_o^i$, being $\rho_o = \sum_i \rho_o^i$ the total material density of the tissue as the sum over all $i$. As mass transport alters the reference density, $\rho_o^i$, assuming that these volume changes are isotropic, it leads to the following growth kinematics $\nabla \cdot \boldsymbol{v}^i - \frac{\dot{\rho}_o^i}{\rho_{i\,\mathrm{orig}}^i}$ where $\boldsymbol{v}$ is the velocity of the material points, $\rho_{i\,\mathrm{orig}}^i$ means the original concentration of a species in the undeformed configuration.[13] It has been assumed that monocyte and macrophage sizes (before ingesting oxydized LDL) as well as cytokine, LDL and oxydized LDL sizes are small in comparison with the sizes of foam cells and SMCs.[6] Thus the isotropic growth of the atheroma plaque can be estimated as[13]

$$\nabla \cdot \boldsymbol{v} = \frac{\partial C\mathrm{F,w}}{\partial t}\mathrm{Vol}_{\mathrm{foamcell}} + \frac{\partial \Delta C_{\mathrm{S,w}}}{\partial t}\mathrm{Vol}_{\mathrm{SMC}} + \frac{\partial C_{G,\mathrm{w}}}{\partial t}\frac{1}{\rho_G} \tag{14}$$

where $\Delta C_{\mathrm{S,w}}$ is the variation of both contractile and synthetic SMCs with respect to the considered initial concentration of these species, $\mathrm{Vol}_{\mathrm{foamcell}} = \frac{4}{3}\pi {R_F}^3$ and $\mathrm{Vol}_{\mathrm{SMC}} = \frac{4}{3}\pi {R_{\mathrm{SMC}}}^2 l_{\mathrm{SMC}}$ are the volume of one foam cell and one SMC, respectively, which can be estimated knowing the radius of a foam cell $R_F$ and a SMC $R_{\mathrm{SMC}}$, and $\rho_G$ the density of the collagen. The foam cell has been considered as spherical and the SMC shape as ellipsoidal.[42]

### *Boundary and Initial Conditions*

#### *Fluid*

A given axial parabolic velocity profile is imposed at the inlet of the artery, $u_f^z = 2u_0\left(1 - \left(\frac{r}{R}\right)^2\right)$, where $u_0$ is the mean inlet velocity as the average of the mean diastolic and systolic velocities in the left anterior descending coronary artery,[26] while a given pressure is given at the outlet. $R$ is the internal radius of the artery and $r$ is the radius of the artery at an axial location. Finally, a non-slip boundary condition was applied between the lumen and the endothelium interface.

For the mass transport calculations at the lumen *volume*, a constant concentration boundary condition is used at the lumen *inlet* for LDL and monocytes. A convective flux condition is used to ensure that LDL and monocytes are convected out of the domain with flow $\boldsymbol{N} = -D_{i,l}\nabla C_{i,l} + \boldsymbol{u}_l C_{i,l}$ with $i$ = LDL, m. Finally, an outflow and no flux boundary conditions were applied at the lumen outlet and lumen artery wall interface, respectively.

### *Transmural Plasma Flow Throughout the Artery Wall*

The coupling of the flow dynamics in the artery lumen with that in the arterial wall is achieved by a three pore model. A transmural volumetric flux ($J_v$ $\left(\frac{m}{s}\right)$) through the endothelium is calculated by means of this theory

$$\begin{aligned} J_v = & \underbrace{J_{v,lj}}_{\text{Leakyjunctions}} + \underbrace{J_{v,nj}}_{\text{Normaljunctions}} + \underbrace{J_{v,v}}_{\text{Vesicularpathways}} \\ & = L_{p,lj}\Delta pr + L_{p,nj}\Delta pr, \end{aligned} \tag{15}$$

where $J_{v,lj}$, $J_{v,nj}$ and $J_{v,v}$ are the volume flux through leaky and normal junctions and the vesicular pathway, respectively. Volume flux occurs mainly through normal and leaky junctions,[43,53] therefore, flux through vesicular pathway can be neglected, $J_{v,v} = 0$. $L_{p,nj}$ is the hydraulic conductivity for the normal junction and $L_{p,lj} = \frac{A_p}{S} L_{p,slj}$, the hydraulic conductivity for the leaky junction, where $\frac{A_p}{S} = \frac{4w_l}{R_{cell}} \phi_{lj}$ represents the fraction of the surface area $S$ occupied by the leaky junctions $A_p$, $R_{cell}$ the endothelial cell radius, $w_l$ the half-width of a leaky junction, and $\phi_{lj}$ is defined as the ratio of the area of leaky *junctions* to the area of all the cells.[23,58] $L_{p,slj}$ is the hydraulic conductivity of a single leaky junction. Once $\phi_{lj}$ is known, the transport properties of the leaky junctions can be calculated accordingly. In the presented model, $\phi_{lj}$ is assigned locally at the endothelium as a function of WSS, so $\phi_{lj} = \frac{LC\pi R_{cell}^2}{unitarea}$ where $LC$ is the correlation between the number of leaky cells per unit area of 0.64 mm$^2$ and the number of mitotic cells that is directly related to the WSS, see Olgac *et al.*[44] for more details. The transport properties of the leaky junctions, i.e., hydraulic conductivity, diffusive permeability and the reflection coefficient, are estimated using the pore theory.[15,44] Accordingly, the hydraulic conductivity of a single leaky junction is given by $L_{p,slj} = \frac{w_l^2}{3\mu_0 l_{lj}}$, where $l_{lj}$ is the length of the leaky junction.[23,58] Finally, given all these considerations, the volume flux $J_v$ through a single pathway can be estimated.

*Substances and Cells*

Moreover, at the media-adventitia interface, a constant LDL concentration value of 0.005 times the LDL concentration retained at the *lumen-intima-media* interface was assigned as Meyer *et al.*[40] reported. The lumen artery wall interface coupling of solute dynamics is achieved by a three pore model that takes into account the vesicular pathway, normal endothelial junctions, and leaky junctions. Thus, the solute flux of LDL at the endothelium was defined as a boundary condition by the Kedem–Katchalsky equations.[27] The total LDL solute flux, $J_{s,LDL}$ $\left(\frac{mol}{m^2 s}\right)$, through a single pathway[1,44] is given by

$$J_{s,LDL} = LDL_{dep} \frac{c_l}{1 + \frac{c_l}{C_{LDL}{}^{th}}} (P_{lj} Z_{lj} + J_{v,lj}(1 - \sigma_{f,lj}) + P_v), \tag{16}$$

with $c_l$ being the luminal LDL concentration at the endothelium. The LDL deposition coefficient, which indicates the percentage of LDL particles from the blood flow deposited at the endothelium, is $LDL_{dep}$.[10,44] Furthermore, since the entrance of LDL into the arterial wall can not grow indefinitely, we consider a natural saturation incorporated by the $C_{LDL}{}^{th}$ that occurs when the LDL levels in the blood are pathological (2.7 mg/ml).[48] Finally, $P_{lj}$ is the diffusive permeability of the leaky junction pathway, $\sigma_{f,lj}$ the solvent drag coefficient for the leaky junctions, $P_{lj}$, the diffusive permeability of the leaky junction pathway and $Z_{lj}$ a fractional reduction factor in the solute concentration gradient at the pore entrance.[44] Applying the proportion between the leaky junction pathway and vesicular transport reported by Cancel *et al.*,[7] the permeability of the vesicular pathway $P_v$ can be calculated.

Regarding the boundary conditions of monocytes, insulation conditions were applied at both axial ends of the wall and the media-adventitia interface, and a perpendicular monocyte inflow to the endothelium has been defined. The solute flow dependence on the WSS has been modeled based on the study by Bulelzai and Dubbeldam.[5] The monocytes solute flux per unit of surface, $J_{s,m}$ $(\frac{cells}{m^2 s})$, is modeled as

$$J_{s,m} = \frac{m_r}{1 + \frac{WSS}{WSS_0}} C_{LDL_{ox,w}} C_{m,l} \tag{17}$$

The value of $WSS_0$ designates the WSS at which the growth rate of the monocyte concentration due to the signaling response by the endothelium is reduced by a factor of two compared to the zero wall shear rate response by the endothelium. Since the monocyte captation for the artery wall is due to the presence of oxidized LDL in the intima, the right hand side of Eq. (17) includes this term $C_{LDL_{ox,w}}$. The factor $m_r$ is a constant which determines the rate at which monocytes enter the intima for small WSS and per mol/m$^3$ of oxidized LDL.[13]

Finally, insulation boundary conditions were applied at both axial ends of the artery wall, where the flux of substances and cells are defined as $N = -D_{i,w} \nabla C_{i,w} + \boldsymbol{u}_w C_{i,w}$, with $i = LDL,\ LDL_{ox},\ m,\ M$.

For the sake of clarity, the values and physiological meaning of the parameters are given in Table 1.

## GEOMETRICAL MODEL AND MESH

A commercial FE code, COMSOL Multiphysics, (COMSOL Inc.), was used to implement the model. Then, a computational geometry corresponds to an idealized axisymmetric representation of a left descending coronary artery with general dimensions of 1.85 and 0.1702 mm for the inner radius and arterial wall thickness, respectively, and the length of the model is 60 times the inner radius.[13,44] Furthermore, a stenosis ratio of 55% is included in the geometry. The artery wall is composed of a three-porous-media membrane for the endothelium and one layer which corresponds to the intima and media layers together.

**TABLE 1. List of parameters related to the biological model.**

| Parameter | Description | Value | References |
|---|---|---|---|
| Blood diffusion coefficients | | | |
| $D_{LDL,l}$ | LDL | $5 \times 10^{-12}$ m$^2$/s | 15 |
| $D_{m,l}$ | Monocytes | $1 \times 10^{-10}$ m$^2$/s | 45 |
| Plasma diffusion coefficients | | | |
| $D^{iso}_{LDL,w}$ | LDL in radial direction | $8 \times 10^{-13}$ m$^2$/s | 46 |
| $D^{iso}_{LDL_{ox},w}$ | Oxidized LDL in radial direction | $8 \times 10^{-13}$ m$^2$/s | 46 |
| $D^{iso}_{m,w}$ | Monocytes in radial direction | $8 \times 10^{-15}$ m$^2$/s | 4 |
| $D^{iso}_{M,w}$ | Macrophages in radial direction | $1 \times 10^{-15}$ m$^2$/s | 4 |
| Parameters | | | |
| $d_{LDL}$ | Degradation LDL | $3.0 \times 10^{-4}$ $s^{-1}$ | 18 |
| $d_m$ | Monocytes differentiation | $1.15 \times 10^{-6}$ $s^{-1}$ | 5 |
| $m_d$ | Monocytes natural death | 2.572 s$^{-1}$ | 32 |
| $LDL_{oxr}$ | Oxidized LDL uptaken | $0.0012 \times 10^{-15}$ m$^3$/cell s | 33 |
| $LDL_{dep}$ | LDL deposition | $1 \times 10^{-2}$ $a_l$ | 10 |
| $M_{r1}$ | Oxidized LDL leads to foam cell | $2.83 \times 10^{-11}$ m$^3$/mol s | 63 |
| $m_r$ | Small WSS rate monocytes | $5.5 \times 10^{-4}$ m$^3$/mol day | 13 |
| $M_{r2}$ | Foam cell formation | $9.25 \times 10^{-24}$ m$^3$/cell s | 63 |
| $d_c$ | Cytokines degradation | $2.3148 \times 10^{-5}$ s$^{-1}$ | 64 |
| $C_r$ | Cytokines production | $3 \times 10^{-10}$ m$^3$/s cells | 50 |
| $S_r$ | Contractile SMCs differentiation | $4.16 \times 10^{-8}$ s$^{-1}$ | 9 |
| $m_{S_s}$ | Synthetic SMCs migration | $1 \times 10^{-5}$ s$^{-1}$ | 20 |
| $G_r$ | Synthesis collagen | $2.157 \times 10^{-11}$ g/cells | 62 |
| $d_G$ | Degradation collagen | $3.85 \times 10^{-7}$ s$^{-1}$ | 24 |
| Dimensions | | | |
| $R_{cell}$ | Endothelial cell radius | 15 $\mu$m | 58 |
| $w_l$ | Half-width of a leaky junction | 20 nm | 58 |
| $l_{lj}$ | Leaky junction length | 2 nm | 58 |
| $R_{LDL}$ | LDL radius | 11 nm | 46 |
| $R_F$ | Foam cell radius | 30.24 $\mu$m | 31 |
| $R_{SMC}$ | SMC radius | 7.5 $\mu$m | 39 |
| $l_{SMC}$ | SMC length | 115 $\mu$m | 39 |
| Threshold | | | |
| $C^{th}_{LDL}$ | LDL threshold | 6.98 mol/m$^3$ | 48 |
| $C^{th}_{M,w}$ | Monocytes mitosis threshold | $550 \times 10^9$ cells/mm | 21 |
| Initial conditions | | | |
| $C^0_{LDL,l}$ | Initial lumen LDL concentration | 1.2 mg/ml | 13 |
| $C^0_{m,l}$ | Initial lumen Monocytes concentration | 550 cells/mm | 13,21 |
| $C_{LDL,adv}$ | Adventitia interface LDL concentration | $0.005C_{LDL,int}$ | 40 |
| $C^0_{S_{c,w}}$ | Contractile smooth muscle cells concentration | $29.28 \times 10^{12}$ mol/m$^3$ | 62 |
| Others | | | |
| $\rho_b$ | Blood density | 1050 kg/m$^3$ | 41 |
| $\mu_b$ | Viscosity density | 0.0035 Pa s | 41 |
| $\rho_p$ | Plasma density | 1000 kg/m$^3$ | 41 |
| $\mu_p$ | Plasma density | 0.001 Pa s | 41 |
| $\kappa_w$ | Darcian artery permeability | $1.2 \times 10^{-18}$ m$^2$ | 56 |
| $\epsilon$ | Intima-media porosity | 0.96 | 1 |
| | | $1.92 \times 10^{11}$ m/s | 44 |
| | | 1 g/ml | 47 |
| | | $1.19 \times 10^{-11}$ m/s | 54 |
| $u_0$ | Mean artery inlet velocity | 0.24 m/s | 26 |
| $\sigma_{f,lj}$ | Drag coefficient of a leaky junction | 0.5682 | 44 |
| $\Delta pr$ | Endothelial pressure difference | 17.5 mmHg | 44,54 |
| $WSS_0$ | Reference WSS | 1 Pa | 5 |

The plasma diffusion coefficients correspond to the isotropic case $D^r_{i,w} = D^z_{i,w}$.

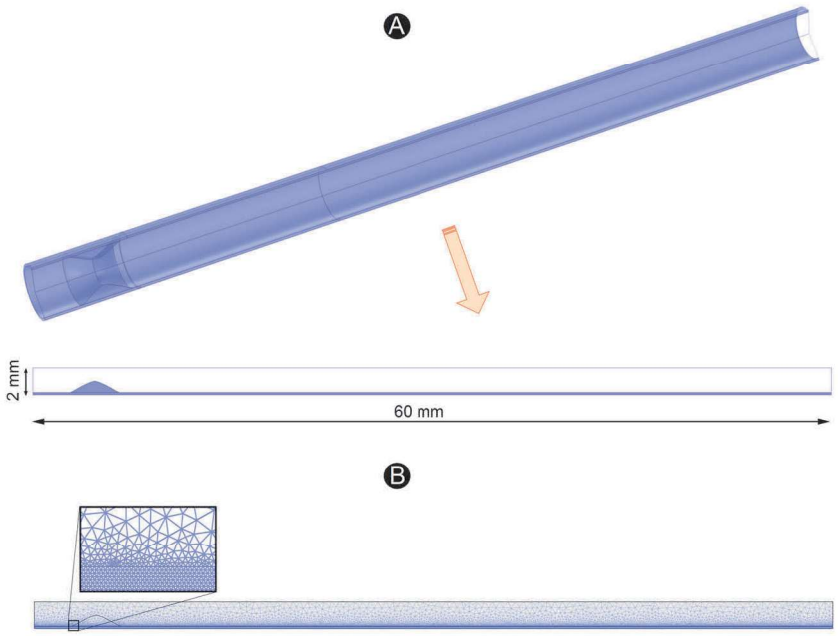


**FIGURE 2. (a) 3D idealized geometry of an atherosclerotic coronary artery stenosed 55% of its area in order to obtain areas of flow recirculation and longitudinal section of this artery where the dashed center line represents the symmetry axis. (b) Longitudinal section of the used mesh, showing a detail of the mesh at the interface between lumen and endothelium.**

**TABLE 2. LDL transport properties for the different cases.**

| Case | $D^r_{LDL,w}$ ($m^2/s$) | $D^z_{LDL,w}$ ($m^2/s$) | $\gamma$ |
|---|---|---|---|
| Case 1 | $8 \times 10^{-13}$ | $8 \times 10^{-13}$ | 1 |
| Case 2 | $8 \times 10^{-13}$ | $8 \times 10^{-14}$ | 0.1 |
| Case 3 | $8 \times 10^{-14}$ | $8 \times 10^{-13}$ | 10 |
| Case 4 | $8 \times 10^{-15}$ | $8 \times 10^{-13}$ | 100 |
| Case 5 | $8 \times 10^{-13}$ | $2.4 \times 10^{-12}$ | 3 |
| Case 6 | $8 \times 10^{-13}$ | $5.2 \times 10^{-12}$ | 6.5 |
| Case 7 | $8 \times 10^{-13}$ | $8 \times 10^{-12}$ | 10 |
| Case 8 | $8 \times 10^{-13}$ | $8 \times 10^{-11}$ | 100 |
| Case 9 | $4 \times 10^{-13}$ | $4 \times 10^{-12}$ | 10 |
| Case 10 | $16 \times 10^{-13}$ | $16 \times 10^{-12}$ | 10 |
| Case 11 | $8 \times 10^{-13}$ | $8 \times 10^{-13}$ | 1 |

Note that $D^z_{i,w} = \gamma D^r_{i,w}$ was also considered for oxidized LDL, monocytes and macrophages, except for Case 11 where $D^r_{LDL_{ox,w}} = D^z_{LDL_{ox,w}} = 0$.

The adventitia layer has been modeled as a boundary condition. Figure 2a shows the coronary artery model used and the axisymmetric section.

The lumen and the arterial wall were meshed with 32848 and 48610 triangular elements, Fig. 2b. Furthermore, grid independence tests were performed successfully for both fluid flow and LDL transport calculations.[13]

## TRANSMURAL TRANSPORT PROPERTIES

Several authors computed the macromolecular transport of the LDL along the arterial wall,[1,12,28,29,44,52,60] however the diffusion properties were considered identical for radial and longitudinal directions of the wall, i.e., isotropic diffusion. Due to the structure of the arterial wall, there is a one or two-order of magnitude difference between the diffusion properties in axial and radial directions[25,35] $D^z_{i,w} = \gamma D^r_{i,w}$. This ratio was analytically estimated by Yuan *et al.*[61] as $\gamma \approx 3$. In this work, we analyze the effect of $\gamma$ on the LDL transport and the growth of atheroma plaque. We change this value from non-physiological conditions $\gamma = 0.1$ to $\gamma = 100$ using intermediate values corresponding to isotropic condition $\gamma = 1$, taken as the baseline model or case 1, or the reported value $\gamma = 3$, see Table 2. Regarding the LDL diffusion coefficient of the media $D^r_{LDL,w}$, we consider the baseline value proposed by Huang *et al.*[22] and used by Olgac *et al.*[44] of $8 \times 10^{-13}$ $m^2/s$. This value is similar to the one estimated by Baldwing *et al.*[3] as $1.1 \times 10^{-13}$ $m^2/s$. However, other authors consider different values, as Vafai works where an isotropic value of $5 \times 10^{-14}$ $m^2/s$[1,12,29,59] was considered. For this reason, we also study the influence of decreasing the radial diffusion of the LDL as $D^r_{LDL,w} = 8 \cdot 10^{-14}$ $\frac{m^2}{s}$, see also Table 2.

The results for the normalized LDL concentration are obtained numerically and compared with the experimental work of Meyer *et al.*[40] and Curmi *et al.*[14] where the transmural distribution of relative concentrations of LDL across the wall were studied *in vitro* in freshly excised rabbit thoracic aorta held at *in vivo* length and pressurized at 70, 120, or 160 mmHg for 30 min and 2 h, respectively.

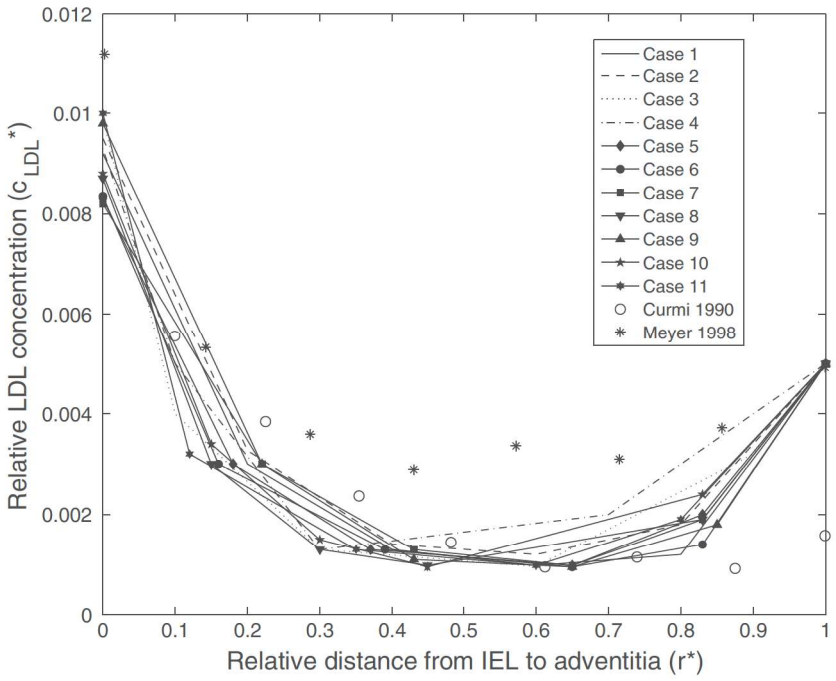


**FIGURE 3. Computed normalized-averaged LDL concentration profile ($C^*_{LDL,w} = C_{LDL,w}/C^0_{LDL,I}$) in the media at transmural pressure of 70 mmHg for the different considered cases and for the experimental data of Curmi *et al.*[14] and Meyer *et al.*[40] $r^*$ is the distance from the endothelium normalized by the thickness of the arterial wall.**

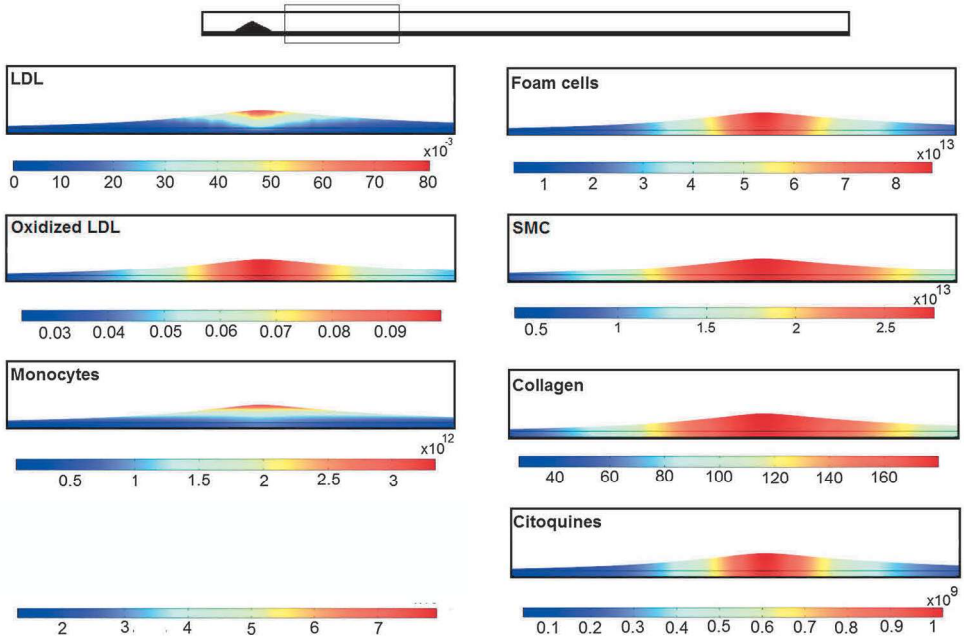


**FIGURE 4. Spatial concentration distribution of the cells and substances along the vessel wall for case 1 (baseline model, $\gamma = 1$). LDL, oxidized LDL and cytokines are in mol/m$^3$; monocytes, macrophages, foam cells and SMC are in cell/m$^3$ and collagen in g/m$^3$.**

## RESULTS

A comparison between the LDL wall concentration profiles obtained by our simulations at a point where the WSS reaches a constant value downstream the stenosis and those observed by Meyer *et al.*[40] and Curmi *et al.*[14] are shown in Fig. 3. The profiles are in good agreement, with the exception of the measurement location closest to the endothelium. The results are closer to Curmi *et al.*[14] data than Meyer *et al.*[40].

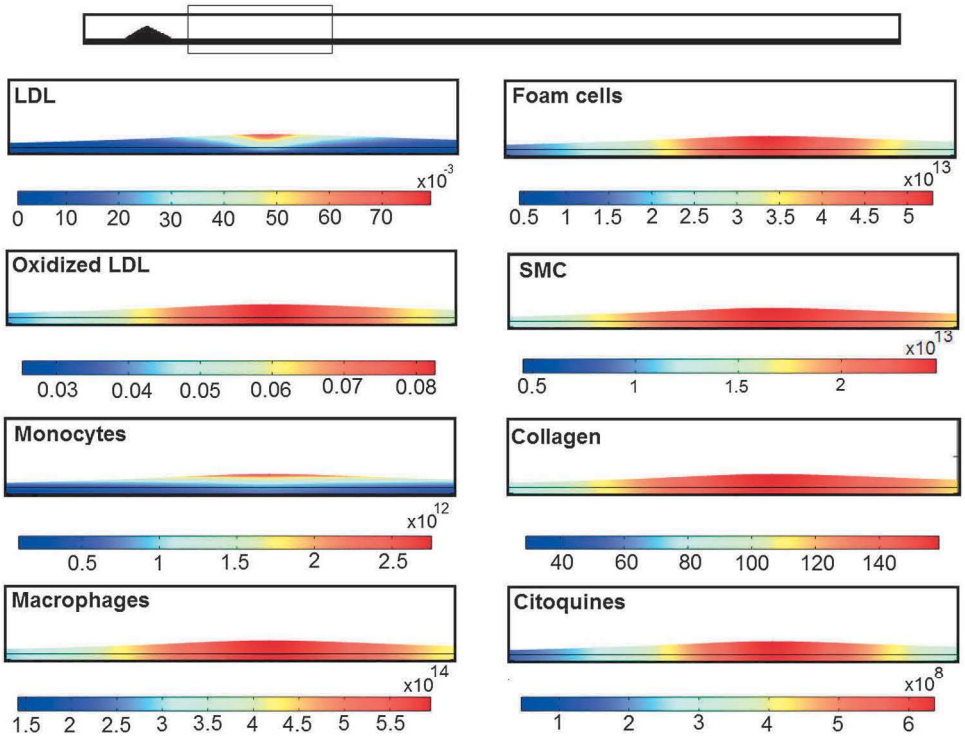


**FIGURE 5. Spatial concentration distribution of the cells and substances along the vessel wall for case 7 (physiological model, $\gamma = 10$). LDL, oxidized LDL and cytokines are in mol/m$^3$; monocytes, macrophages, foam cells and SMC are in cell/m$^3$ and collagen in g/m$^3$.**

**TABLE 3. Stenosis area ratio (%) for each analyzed case.**

| Case | Stenosis area ratio (%) |
|---|---|
| Case 1 | 50 |
| Case 2 | 57 |
| Case 3 | 51 |
| Case 4 | 43 |
| Case 5 | 43 |
| Case 6 | 39 |
| Case 7 | 33 |
| Case 8 | 19 |
| Case 9 | 21 |
| Case 10 | 13 |
| Case 11 | 47 |

This factor represents the ratio between the area occupied by the grown atheroma plaque divided by the lumen area of a healthy artery.

The concentration value at the media-adventitia interface is fixed by the imposed constant concentration boundary condition. Its value is given by that measured by Meyer *et al.*[40]. There is not a strong influence of the anisotropic transmural properties on LDL distribution along the artery when WSS reaches a constant value.

The spatial concentration distribution of the cells and substances for case 1 (baseline model) and case 7 (physiological model) after 10 years are shown in Figures 4 and 5. The simulated advanced lesions grow progressively in size due to the increasing mass of substances and cells. All substances and cells are concentrated close to the lower shear stress zone,[13] being the low WSS the trigger to the plaque initiation process. In particular, due to the continuum flux of LDL and monocytes thought lumen, these substance and cells are strongly concentrated in the intima-media layer. Oxidized LDL, macrophages, cytokines and foam cells (lipid derived from macrophages death) accumulate mainly in the upper side of the media. However, SMCs and collagen are distributed through the whole media. These results are in agreement with the clinical evidences.[19,34,55] When transport properties are anisotropic ($\gamma = 10$), there is a more uniform axial distribution of the substances and cells and consequently the plaque grows slower in the radial direction. The stenosis ratio was 50% and 33% for cases 1 and 7, respectively, see Table 3.

The effects of transmural properties on the plaque growth are studied. Figure 6a illustrates the influence of the anisotropic diffusion on the LDL concentration along the plaque. For the non-physiological case where $\gamma = 0.1$ (case 2, more diffusion in radial direction than longitudinal one), there is a strongly concentration of LDL on the intima-media layer and the plaque grows. Using anisotropic physiological diffusion properties (cases 5, 6 and 7), there is a more uniform distribution

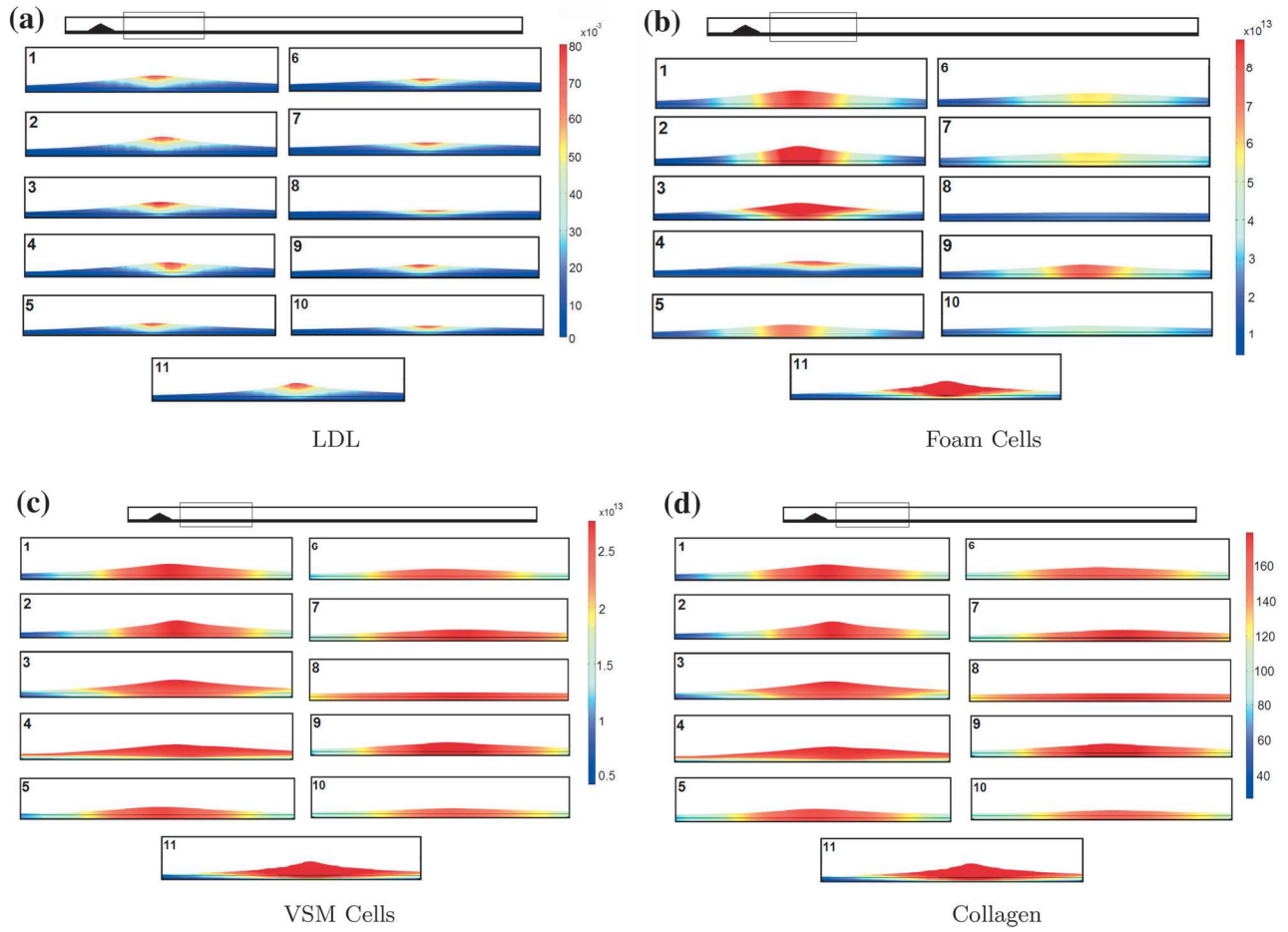


**FIGURE 6. Spatial concentration distribution of the LDL (mol/m$^3$), foam cells and SMC (cell/m$^3$) and collagen (g/m$^3$) for each analyzed cases.**

of the LDL and there are no relevant differences between models. Decreasing one order of magnitude the diffusion properties until $8 \times 10^{-14}$ m$^2$/s in radial direction and $8 \times 10^{-13}$ m$^2$/s in longitudinal one (case 3), increases the LDL concentration and the growth of the plaque respect to physiological values (Table 3). In fact, there are no differences in the distribution respect to the isotropic case. When the difference on the diffusion coefficient between longitudinal direction respect to the radial direction is unphysiological ($\gamma = 100$, case 8), there is no localized plaque growth although the LDL distribution is similar to the previous one. The cases with higher longitudinal diffusion coefficient (cases 5–10) present a slower growth rate than the rest of cases (cases 1–4 and case 11).

Figure 6b depicts the influence of the anisotropic diffusion on the foam cell distribution. Changes in diffusion properties have a strongly influence in concentration and distribution of these cells. Decreasing $\gamma$ produces a higher concentration of the foam cells close to the intima-media layer contributing to form a more vulnerable plaque (cases 1, 2, 3 and 9). On the contrary, when $\gamma = 10 \div 100$, although high concentration of LDL is found, there are limited foam cells showing a predisposition to evolve to a fibrotic plaque (case 4 and 7). Note that for the extreme example or null diffusion of oxidized LDL (case 11), the plaque is mainly lipidic, showing the relevance of the diffusion properties of oxidized LDL on the plaque growth. Finally, Figs. 6c and 6d show the effect of transmural transport properties on the SMCs distribution and collagen concentration. As expected, there is much less influence of the diffusion properties on the SMCs and collagen distribution due their diffusion was neglected (see Eqs. (12) and (7), respectively). Changes in concentration or distribution of SMCS are very related to changes on cytokines, results are not shown.

## DISCUSSION

In a previous study,[13] a mathematical model of atheroma plaque formation and development in coronary arteries using isotropic transmural diffusion properties was proposed. Our current approach is focused on the process of plaque initiation and intima-media thickening rather than severe plaque progression and potential rupture. The effect of transport properties, in particular the anisotropy of diffusion properties of the artery, on the plaque formation and development is investigated using this mathematical model.

The computed LDL concentration profile throughout the arterial wall and the results of Meyer *et al.*[40] and Curmi *et al.*[14] at 70 mmHg is in good agreement with the exception of the experimental measurement point that is closer to the endothelium. For the baseline model (case 1) similar results were obtained by other authors in LDL transport models.[1,12,28,29,44,52,60] These results could be used as a validation of the macromolecule and cell transport model. Although the developed model is relatively simple, it captures some of the main features of atherosclerosis lesions formation. The model is also in accordance with the clinical hypothesis that correlates atherosclerosis occurrence with low WSS. However, although the results obtained are reasonable in terms of the biological process of atheroma plaque growth, these results can not be quantitatively validated since the appropriate experiments which directly measured the concentration of each species at the human artery wall over time are not currently available.

There is not a great influence of the anisotropic transmural properties on LDL distribution through the artery wall in the zone where WSS reaches a stabilized and uniform value. This effect is also observed in the location where the new plaque is formed, see Fig. 6a. Similar results were obtained for SMCs and collagen distribution, since there is few influence of the diffusion material properties on SMCs and collagen concentrations due to diffusion was neglected for these cells and substance (Figs. 6c and 6d). On the contrary, foam cells distribution strongly changes depending on the value of the radial diffusion coefficient of the substances $D^{r}$ and the ratio $\gamma = D^{z}_{i,w}/D^{r}_{i,w}$. Decreasing $\gamma$ leads to a higher concentration of the foam cells close to the intima-media layer. On the contrary, when $\gamma = 10 \div 100$, although a high concentration of LDL, there is a significant reduction of foam cells. Due to foam cell is associated to a necrotic core, the final distribution of foam cells is critical for a plaque to evolve to a vulnerable (cases 1, 2, 3 and 9) or fibrotic plaque (case 4 and 7). Therefore, the transmural properties could be an important factor for the development of fatty or fibrotic plaques. However, this is an hypothesis that should be validated. The axial diffusivity of LDL mainly affects foam cell far more than SMCs or collagen concentration. The reason for this is not clear. Both the formation of foam cells and cytokines, according to the given models, depend on the product of oxidized LDL and Macrophages (eqs 6 and 10). Macrophages come from monocytes, whose production is also proportional to oxidized LDL. Thus both foam cell and cytokine formation are essentially quadratic in oxidized LDL. The region of low WSS has more leaky junctions and thus more LDL, which quickly becomes oxidized LDL. Thus increasing axial LDL diffusion will have a large effect by getting rid of the LDL before it produces its downstream products. If its degradation is not too fast, it seems one might expect an effect on cytokine that is similar to that on foam cell concentration. In contrast, total muscle cell production (here *via* chemotaxis) and the production of its product, collagen, do not depend directly on LDL or oxidized LDL, but rather have only a linear, indirect acceleration at high cytokines that is totally muted by its product with synthetic SMCs. So one expects a far lower effect of increased axial LDL diffusivity on them.

The presented model considers some important assumptions. First, the endothelium is assumed as a single layer of endothelial cells, which are elongated in the direction of the blood flow. Endothelial cells are interconnected through intercellular junctions. Internal elastic lamina is an impermeable elastic tissue with fenestral pores which lies between the intima and media layers. The processes which lead to atheroma plaque evolution take place mainly in the intima and media layers. Therefore, it should be noted that in the context of arterial mass transport and atheroma plaque formation, the arterial wall refers to the intima and the media layers, with the adventitia as the outer boundary layer (only included in the model as imposed boundary condition). So, most probably a multi-layer model could improve the plaque growth model.[28] Second, this model focuses on purely mechanical factors which promote endothelial dysfunction such as low shear stress.[17] Therefore, in this model the endothelium permeability has been linked to the WSS distribution along the internal artery wall. This study does not take into account the mechanotaxis of the atheroma plaque growth process since the WSS has been considered as the only triggered factor for atherosclerosis initiation, and the cyclic stretch effects of vessel compliance, curvature, pulsatile blood flow or cardiac motion have been neglected. The arterial mass transport is coupled with both the bulk blood flow in the lumen and the transmural flow in the wall, therefore fluid dynamic models and solute dynamic models have been included.

Additionally, the arterial wall can be treated as a porous medium. As such, it is of great importance to characterize the porous media transport models used in describing biological phenomena. Most human tissues can be modeled as porous media as they are composed of dispersed cells separated by connective voids where blood flows.[29] Another important limitation in this study is the supposition of arterial wall as rigid. Additional effort is needed to have a fully coupled time-dependent fluid flow, mass transfer growth and flexible structure with a multi-layered arterial wall solid and used this model in actual arterial geometries. Third, the model parameters were obtained from a wide variety of experiments on many different human or animal models. However, a few parameters have been estimated attending the order of magnitude of these parameters and making choices that gave biologically reasonable results. Fourth, a sensitive study of the parameters used in the growth model in order to assess the influence on the obtained results should be executed. Fifth, an idealized straight geometry based on the human left anterior descending (LAD) coronary artery has been used to perform the analysis, however the achieved recirculation zones are comparable to those that are developed at arterial bifurcations.[44] In spite of these limitations, the development of personalized in-silico technologies for plaque growing is a good choice to approach some of the questions that atherosclerosis disease still presents.

## ACKNOWLEDGMENTS

Financial support for this research was provided by the Spanish Ministry of Economy and Competitiveness through research projects DPI2013-44391; and the Instituto de Salud Carlos III (ISCIII) through the CIBER initiative.

## CONFLICT OF INTEREST

Neither author has a financial or proprietary interest in any material or method mentioned. All authors read and approved the final manuscript. The authors have no conflicts of interest to disclose.

## REFERENCES

[1]Ai, L., and K. Vafai. A coupling model for macromolecule transport in a stenosed arterial wall. Int. *J. Heat Mass Transf.* 49:1568–1591, 2006.

[2]Baggiolini, M. Chemokines and leukocyte traffic. *Nature* 392:565–568, 1998.

[3]Baldwin, A. L., L. M. Wilson, I. Gradus-Pizlo, R. Wilensky, and K. March. Effect of atherosclerosis on transmural convection and arterial ultrastructure. Implications for local intravascular drug delivery. *Arterioscler. Thromb.* 17:3365–3375, 1997.

[4]Budu-Grajdeanu, P., R. C. Schugart, A. Friedman, C. Valentine, A. K. Agarwal, and B. H. Rovin. A mathematical model of venous neointimal hyperplasia formation. *Theor. Biol. Med. Model.* 1:5–2, 2008.

[5]Bulelzai, M. A. K. and Johan L. A. Dubbeldam. Long time evolution of atherosclerotic plaques. *J. Theor. Biol.* 297:1–10, 2012.

[6]Calvez V., A. Ebde, N. Meunier, and A. Raoult. Mathematical modelling of the atherosclerotic plaque formation. *ESAIM Proc.* 28:1–12, 2009.

[7]Cancel, L. M., A. Fitting, and J. M. Tarbell. In vitro study of LDL transport under pressurized (convective) conditions. *Am. J. Physiol. Heart Circ. Physiol.* 293:126–132, 2007.

[8]Cavaillon, J. M. Cytokines and macrophages. *Biomed. Pharmacother.* 48:445–453, 1994.

[9]Chamley-Campbell, J. H., G. R. Campbell, and Ross R. Phenotype-dependent response of cultured aortic smooth muscle to serum mitogens. *J. Cell Biol.* 89:379–383, 1981.

[10]Chang, C. L. Lipoprotein lipase in the arterial wall: regulation by dietary fatty acids. PhD thesis, Columbia University, 2011.

[11]Chatzizisis, Y. S., A. P. Antoniadis, J. J. Wentzel, and G. D. Giannoglou. Vulnerable plaque: the biomechanics of matter. *Arterioscler* 236:351–352, 2014.

[12]Chung, S. and K. Vafai. Low-density lipoprotein transport within a multi-layered arterial wall. Effect of the atherosclerotic plaque/stenosis. *J. Biomech.* 46:574–585, 2013.

[13]Cilla, M., E. Peña, and M. A. Martínez. Mathematical modelling of atheroma plaque formation and development in coronary arteries. *J. R. Soc. Interface* 11:201308661–2013086616, 2014.

[14]Curmi, P. A., L. Juan, and A. Tedgui. Effect of transmural pressure on low density lipoprotein and albumin transport and distribution across the intact arterial wall. *Circ. Res.* 66:1692–1702, 1990.

[15]Curry, F. E.. Mechanics and Thermodynamics of Transcapillary Exchange. Handbook of Physiology. The Cardiovascular System. Microcirculation. Bethesda, MD: American Physiological Society, 1984.

[16]Dabagh, M., P. Jalali and J.M. Tarbell. The transport of LDL across the deformable arterial wall: the effect of endothelial cell turnover and intimal deformation under hypertension.*Am. J. Physiol. Heart Circ. Physiol.* 297(3):H983–H996, 2009.

[17]Davignon, J. and P. Ganz. Role of endothelial dysfunction in atherosclerosis. Circulation, 109:27–32, 2004.

[18]Esterbauer, H., G. Striegl, H. Puhl, and M. Rotheneder. Continuous monitoring of in vitro oxidation of human low density lipoprotein. *Free Radic. Res. Commun.* 6:67–75, 1989.

[19]Finn, A. V., M. Nakano, J. Narula, F. D. Kolodgie, and R. Virmani. Concept of vulnerable/unstable plaque. *Arterioscler. Thromb.* 30:1282–1292, 2010.

[20]Griffin, C. A., L. H. Apponi, K. K. Long, and G. K. Pavlath. Chemokine expression and control of muscle cell migration during myogenesis. *J. Cell Sci.* 123:3052–3060, 2010.

[21]Halim-Khan, F. The Elements of Immunology. New Delhi: Pearson Education India, 2009.

[22]Huang, Y., D. Rumschitzki, S. Chien, and S. Weinbaum. A fiber matrix model for the growth of macromolecular leakage spots in the arterial intima. *Adv. Biol. Heat Mass Transf. HTD* 231:81–92, 1992.
[23]Huang, Z. J. and J. M. Tarbell. Numerical simulation of mass transfer in porous media of blood vessel walls. *Am. J. Physiol. Heart Circ. Physiol.* 273:464–477, 1997.
[24]Humphrey, J. D. Cardiovascular Solid Mechanics: Cells, Tissues, and Organs. New York: Springer-Verlag, 2002.
[25]Hwang, C. W., D. Wu, and E. R. Edelman. Physiological transport forces govern drugdistribution for stent based delivery. *Circulation* 104(7):660–605, 2001.
[26]Iliceto, S., V. Marangelli, C. Memmola, and P. Rizzon. Transesophageal Doppler echocardiography evaluation of coronary blood flow velocity in baseline conditions and during dipyridamole-dipyridamole-induced coronary vasodilation. *Circulation* 83:61–69, 1991.
[27]Kedem, O. and A. Katchalsky. Thermodynamic analysis of the permeability of biological membranes to non-electrolytes. *Biochim. Biophys. Acta* 27:229–246, 1958.
[28]Khakpour, M. and K. Vafai. Critical assessment of arterial transport models. *J. Heat Mass Transf.* 51(3–4):807–822, 2008.
[29]Khaled, A. R. A. and K. Vafai. The role of porous media on modeling flow and heat transfer in biological tissues. *J. Heat Mass Transf.* 46:4989 5003, 2003.
[30]Khamdaengyodtai, P., K. Vafai, P. Sakulchangsatjatai, and P. Terdtoon. Effects of pressure on arterial failure. *J. Biomech.* 45:2577–2588, 2012.
[31]Krombach, F., S. Münzing, A. M. Allmeling, J. T. Gerlach, J. Behr, and M. Dörger. Cell size of alveolar macrophages: an interspecies comparison. *Environ Health Perspect* 105:1261–1263, 1997.
[32]Krstic, R. V. Human microscopic anatomy: an atlas for students of medicine and biology. Berlin: Springer-Verlag, 1997.
[33]Kruth, H. S., W. Huang, I. Ishii, and W. Y. Zhang. Macrophage foam cell formation with native low density lipoprotein. *J. Biol. Chem.* 277:34573–34580, 2002.
[34]Lee, R. T. and P. Libby. The unstable atheroma. *Arterioscler. Thromb.* 17:1859–1867, 1997.
[35]Levin, A. D., N. Vukmirovic, C. W. Hwang, and E. R. Edelman. Specific binding to intracellular proteins determines arterial transport properties for rapamycin and paclitaxel. *Proc. Natl. Acad. Sci. USA* 101(25):9463–9467, 2004.
[36]Lloyd-Jones, D. and the American Heart Association Statistics Committee and Stroke Statistics Subcommittee. Heart disease and stroke statistics-2009 update: A report from the American Heart Association Statistics Committee and Stroke Statistics Subcommittee. *Circulation* 119:21–181, 2009.
[37]Majno, G. and I. Joris. Cells, Tissues and Disease: Principles of General Pathology. Cambridge, MA: Blackwell Science, 1996.
[38]Malek, A. M., S. L. Alper, and S. Izumo. Hemodynamic shear stress and its role in atherosclerosis. *J. Am. Med. Assoc.* 282(1):2035–2042, 1999.
[39]Martini, F. H. Anatomy and Physiology. Chapter 10: Muscle Tissue. Upper Saddle River, NJ: Prentice Hall, 1999.
[40]Meyer, G., R. Merval, and A. Tedgui. Effects of pressure-induced stretch and convection on low-density lipoprotein and albumin uptake in the rabbit aortic wall. *Circ. Res.* 79:532–540, 1996.
[41]Milnor, W. R. Hemodynamics. 2nd Edition. Baltimore, MD: Williams and Wilkins, 1989.
[42]Nakanoa, A., M. Minamiyamab, and J. Sekic. The three-dimensional structure of vascular smooth muscle cells: a confocal laser microscopic study of rabbit mesenteric arterioles. *Asian Biomed.*1:77–86, 2007.
[43]Ogunrinade, O., G. T. Kameya, and G. A. Truskey. Effect of fluid shear stress on the permeability of the arterial endothelium. *Ann. Biomed. Eng.* 30:430–446, 2002.
[44]Olgac, U., V. Kurtcuoglu, and D. Poulikakos. Computational modeling of coupled blood-wall mass transport of LDL: effects of local wall shear stress. *Am. J. Physiol. Heart Circ. Physiol.* 294(2):909 919, 2008.
[45]Petty, H. R., L. M. Smith, D. T. Fearont, and H. M. McConnell. Lateral distribution and diffusion of the C3b receptor of complement, HLA antigens, and lipid probes in peripheral blood leukocytes. *PNAS* 77(11):6587–6591, 1980.
[46]Prosi, M., P. Zunino, K. Perktold, and A. Quarteroni. Mathematical and numerical models for transfer of low-density lipoproteins through the arterial walls: a new methodology for the model set up with applications to the study of disturbed lumenal flow. *J. Biomech.* 38:903–917, 2005.
[47]Sáez, P., E. Peña, M. A. Martínez, and E. Kuhl. Mathematical modeling of collagen turnover in biological tissue. *J. Math. Biol.* 67:1765 1793, 2013.
[48]Schwenke, D. C. and T.E. Carew. Initiation of atherosclerotic lesions in cholesterol-fed rabbits, II: selective retention of LDL vs. selective increases in LDL permeability in susceptible sites of arteries. *Arteriosclerosis* 9:908–918, 1989.
[49]Shanahan, C. M. and P. L. Weissberg. Smooth muscle cell phenotypes in atherosclerotic lesions. *Curr. Opin. Lipidol.* 10:507–513, 1999.
[50]Siogkas, P., A. Sakellarios, T. P. Exarchos, L. Athanasiou, E. Karvounis, K. Stefanou, E. Fotiou, D. I. Fotiadis, K. K. Naka, L. K. Michalis, N. Filipovic, and O. Parodi. Multiscale-patient-specific artery and atherogenesis models. *IEEE Trans. Biomed. Eng.* 58:3464–3468, 2011.
[51]Slager, C. J., J. J. Wentzel, F. J. Gijsen, J. C. Schuurbiers, A. C. Van der Wal, A. F. Van der Steen, and P. W. Serruys. The role of shear stress in the generation of rupture-prone vulnerable plaques. *Nat. Clin. Pract. Cardiovasc. Med.* 2:401–407, 2005.
[52]Stangeby, D. K. and C. R. Ethier. Computational analysis of coupled blood-wall arterial LDL transport. *ASME J. Biomech. Eng.* 124:1–8, 2002b.
[53]Tarbell, J. M. Mass transport in arteries and the localization of atherosclerosis. *Annu. Rev. Biomed. Eng.* 5:79–118, 2003.
[54]Tedgui, A. and M. J. Lever. Filtration through damaged and undamaged rabbit thoracic aorta. *Am. J. Physiol. Heart Circ. Physiol.* 247:784–791, 1984.
[55]VanEpps, J. S. and D. A. Vorp. Mechanopathobiology of atherogenesis: a review. *J. Surg. Res.* 142:202–217, 2007.
[56]Vargas, C. B., F. F. Vargas, J. G. Pribyl, and P. L. Blackshear. Hydraulic conductivity of the endothelial and outer layers of the rabbit aorta. *Am. J. Physiol. Heart Circ. Physiol.* 236:53–60, 1979.
[57]Wang, J. C., S. L. Normand, L. Mauri, and R. E. Kuntz. Coronary artery spatial distribution of acute myocardial infarction occlusions. *Circulation* 110(3):278–284, 2004.
[58]Weinbaum, S., G. Tzeghai, P. Ganatos, R. Pfeffer, and Chien S. Effect of cell turnover and leaky junctions on arterial macromolecular transport. *Am. J. Physiol. Heart Circ. Physiol.* 248:945–960, 1985.

[59]Yang, N. and K. Vafai. Modeling of low-density lipoprotein (LDL) transport in the artery. Effects of hypertension. *J. Heat Mass Transf.* 49:850–867, 2006.
[60]Yang, N. and K. Vafai. Low-density lipoprotein (LDL) transport in an artery—a simplified analytical solution. *J. Heat Mass Transf.* 51:497–505, 2008.
[61]Yuan, F., S. Chien, and S. Weinbaum. A new view of convective–diffusive transport processes in the arterial intima. *ASME J. Biomech. Eng.* 113:314–329, 1991.
[62]Zahedmanesh, H., H. Van Oosterwyck, and C. Lally. A multi-scale mechanobiological model of in-stent restenosis: decipheringthe role of matrix metalloproteinase and extracellular matrix changes. *Comput. Methods Biomech. Biomed. Eng.*, 2012. doi:10.1080/10255842.2012.716830.
[63]Zhao, B., Y. Li, C. Buono, S. W. Waldo, N. L. Jones, M. Mori, and H. S. Kruth. Constitutive receptor-independent low density lipoprotein uptake and cholesterol accumulation by macrophages differentiated from human monocytes with macrophage-colony-stimulating factor (M-CSF). *J. Biol. Chem.* 281:15757–15762, 2006.
[64]Zhao, W., C. A. Oskeritzian, A. L. Pozez, and L. B. Schwartz. Cytokine production by skin-derived mast cells: endogenous proteases are responsible for degradation of cytokines. *J. Immunol.* 175(4):2635–2642, 2005.
[65]Zlotnik, A. and O. Yoshie. Chemokines: a new classification system and their role in immunity. *Immunity* 12:121–127, 2000.